ISSN 1672-9145 **Acta Biochimica et Biophysica Sinica** 2007, **39**(5): 335–343 **CN** 31-1940/Q

Crystal Structures of Human Dipeptidyl Peptidase IV in its Apo and Diprotin B-complexed Forms

Hajime HIRAMATSU[1], Kiyoshi KYONO[1], Atsushi YAMAMOTO[1], Kazuhiko SAEKI[1], Hideaki SHIMA[2], Shigeru SUGIYAMA[3,4], Koji INAKA[3], and Ryo SHIMIZU[1]*

[1] *Tanabe Seiyaku Co. Ltd, Osaka 532-8505, Japan;*
[2] *Aphoenix Inc., Tokyo 150-0002, Japan;*
[3] *Maruwa Food Industries Inc., Nara 639-1123, Japan;*
[4] *Mol Logics Inc., Kyoto 619-0237, Japan*

Abstract Dipeptidyl peptidase IV (DPPIV), which belongs to the prolyl oligopeptidase family of serine proteases, is known to have a variety of regulatory biological functions and has been shown to be implicated in type 2 diabetes. It is therefore important to develop selective human DPPIV (hDPPIV) inhibitors. In this study, we determined the crystal structure of apo hDPPIV at 1.9 Å resolution. Our high-resolution crystal structure of apo hDPPIV revealed the presence of sodium ion and glycerol molecules at the active site. In order to elucidate the hDPPIV binding mode and substrate specificity, we determined the crystal structure of hDPPIV-diprotin B (Val-Pro-Leu) complex at 2.1 Å resolution, and clarified the difference in binding mode between diprotin B and diprotin A (Ile-Pro-Ile) into the active site of hDPPIV. Comparison between our crystal structures and the reported apo hDPPIV structures revealed that positively charged functional groups and conserved water molecules contributed to the interaction of ligands with hDPPIV. These results are useful for the design of potent hDPPIV inhibitors.

Key words dipeptidyl peptidase IV; diprotin B; serine protease; crystal structure; water molecule

Dipeptidyl peptidase IV (DPPIV, EC 3.4.14.5), which belongs to the prolyl oligopeptidase family of serine proteases, was first identified by Hopsu-Havu and Glenner in rat liver homogenates as a glycylprolyl naphtylamidase [1]. DPPIV is widely expressed in a number of mammalian tissues including differential epithelial cells, endothelial cells, and lymphocytes [2].

Human DPPIV (hDPPIV) is a cell surface type II membrane glycoprotein, also called adenosine deaminase binding protein or T cell activation marker CD26 [3]. hDPPIV is a single polypeptide chain of 766 amino acids and consists of four domains: an N-terminal cytoplasmic domain, a trans-membrane domain, a β-propeller domain, and an α/β-hydrolase domain [4]. hDPPIV, which cleaves dipeptides with penultimate Pro or Ala from the N-terminus of polypeptides, is known to have a variety of biological functions, especially in regulation of the activity of multiple hormones, chemokines, neuropeptides, and peptides of the glucagon family, and has been implicated in type 2 diabetes [5]. It has been reported that hDPPIV hydrolyses the glucagon-like peptide 1 and glucose-dependent insulinotropic polypeptide, two important insulin-releasing incretins [6], whose degradation enhances insulin secretion and improves glucose tolerance in mice [7]. Therefore, selective inhibitors of hDPPIV are expected to be valuable therapeutic agents for type 2 diabetes. Some hDPPIV inhibitors have already been used in clinical trials [8].

A number of crystal structures of human and porcine DPPIV both in apo form and complexed with various small molecules have been reported [9–23]. We have previously reported the crystal structure of apo hDPPIV at 2.6 Å resolution [9] and that of the hDPPIV-diprotin A (Ile-Pro-Ile) complex at 2.2 Å resolution [10].

Water molecules are important in stabilizing high-order structures of proteins [24], catalytic efficiency [25] and

Received: December 29, 2006 Accepted: February 27, 2007
*Corresponding author: Tel, 81-6-63002568; Fax, 81-6-63002528; E-mail, ryo@tanabe.co.jp

DOI: 10.1111/j.1745-7270.2007.00289.x

molecular recognition [26]. Accurate identification of water molecules around a target protein gives important information to design ligands that interact with that specific protein. To precisely identify water molecules in a protein, the crystal structure of the protein has to be determined at high resolution.

In this study, we determined the crystal structure of apo hDPPIV at 1.9 Å resolution and provided insights for the design of potent hDPPIV inhibitors. In addition, to further elucidate the hDPPIV binding mode and substrate specificity, we determined the crystal structure of hDPPIV complexed with diprotin B (Val-Pro-Leu) at 2.1 Å resolution. Diprotin B, known as a slowly hydrolysable substrate of DPPIV [27], was isolated from culture filtrates of *Bacillus cereus* BMF673-RF1 [28].

Materials and Methods

Protein expression, purification, and crystallization

hDPPIV was expressed by a baculovirus system and chromatographically purified as previously reported [29]. Apo hDPPIV and hDPPIV-diprotin B complex crystals were obtained by the same crystallization method as described before [10,29]. These crystals showed the same crystal form as described previously [10]. Diprotin B was synthesized by Thermo Fisher Scientific, Inc. (Massachusetts, USA).

Data collection and processing

X-ray diffraction data for apo hDPPIV and hDPPIV-diprotin B complex crystals were collected with an imaging plate detector (R-AXIS V; Rigaku, Tokyo, Japan) and a charge-coupled device (Jupiter 210; Rigaku), respectively, using the synchrotron radiation source at SPring-8 (BL32B2, beamline of Pharmaceutical Consortium for Protein Structure Analysis; PCProt, Hyogo, Japan). For X-ray data collection at 100 K, a cryo-protectant solution was prepared as reservoir solution by adding 15% (*V*/*V*) glycerol. Apo hDPPIV and hDPPIV-diprotin B complex crystals diffracted beyond 1.9 Å and 2.1 Å resolution, respectively. Imaging data were processed and scaled with the programs MOSFLM [30] and SCALA in the CCP4 package [31]. Statistics for data collection are summarized in **Table 1**.

Table 1 Summary of crystallographic data and structure refinement statistics for human dipeptidyl peptidase IV

Parameter	Apo	Diprotin B
Data collection		
Beamline	BL32B2/SPring-8	BL32B2/SPring-8
Detector	R-AXIS V	Jupiter 210
Crystallographic data		
Space group	$P2_12_12_1$	$P2_12_12_1$
Cell dimensions		
a (Å)	118.12	118.05
b (Å)	125.94	126.40
c (Å)	136.92	137.38
Resolution (Å)	1.9 (2.00–1.90)	2.1 (2.21–2.10)
Number of observations	1,066,448	296,786
Number of unique reflections	159,535	110,310
R_{merge} (%)	8.8 (36.9)	8.2 (37.5)
I/sigma	6.2 (2.0)	5.8 (2.0)
Redundancy	6.7 (5.2)	2.7 (2.4)
Completeness (%)	99.4 (96.5)	92.7 (88.8)
Structure refinement statistics		
Resolution range (Å)	20.0–1.9	20.0–2.1
R-factor (%)	21.9	22.8
R_{free}-factor (%)	24.5	26.4
Average B-factor (Å^2)	23.9	28.6
R.m.s. deviation		
Bond length (Å)	0.004	0.004
Bond angle (°)	1.27	1.26
Number of atoms		
Non-hydrogen protein atoms	11,944	11,944
Peptide	–	46
Sugar	286	294
Water	1486	1018
Ions	4	2
Glycerol	12	–

Values in parentheses refer to the highest resolution shell. –, No atoms; r.m.s., root mean square. R_{merge} (%)=$\Sigma_{hkl}\Sigma_i|I\ (hkl)I-<I\ (hkl)>|/\Sigma_{hkl}\Sigma_i\ I\ (hkl)_i$.

Structural determination and refinement

The structure of apo hDPPIV was solved by the molecular replacement method using the structure of apo hDPPIV [9] as a search model with the program CNX [32]. Manual model rebuilding was performed using the program QUANTA (Accerlys, San Diego, USA) and subsequent interactive refinement (initially performed as a rigid body refinement) was conducted using the program CNX. After simulated annealing refinement, the model was manually fitted on an electron density map and further refinement was performed. The electron density of the mol-

ecule was relatively clear except for the trans-membrane region around Ala37. Water molecules were included under the criteria that they were in chemically acceptable positions and lay in electron density in 2|Fo| – |Fc| maps, and that their B-factor values were lower than 50 Å^2. The same refinement procedure was applied to the structure of the hDPPIV-diprotin B complex. The structures of apo hDPPIV and hDPPIV-diprotin B complex were refined at 1.9 Å and 2.1 Å resolution, respectively. A summary of refinement statistics for the two structures is shown in **Table 1**. The structures were validated with the program PROCHECK [33]. The program LSQMAN from Uppsala Software Factory (Uppsala, Sweden) was used to calculate r.m.s. deviations for superimposition of the molecules [34]. The figures in this paper were generated using the program QUANTA.

Calculation method of Na^+-specific valence

The Na^+-specific valence of each molecule was calculated using **Equation 1** [35–38]:

$$V_{Na^+} = \sum_{j=1}^{M} V_j = \sum_{j=1}^{M} \left(R_j / R_0 \right)^{-N} \quad 1$$

where V_j is the valence contributed by the jth ligating oxygen in the coordination shell located at a distance R_j, and M is the total number of oxygen atoms within 4.0 Å. The parameters R_0 and N translate bond length into bond strength, or valence, and are specific for a given metal ion-oxygen pair. The values for the Na^+–O pair are R_0= 1.622 Å and N=4.29 [36].

Results and Discussion

Crystal structure of apo hDPPIV

The crystal structure of apo hDPPIV revealed two molecules of hDPPIV containing two glycerol molecules and four sodium ions in an asymmetric unit. Each hDPPIV molecule consisted of 729 amino acid residues. Although we have previously reported the crystal structure of apo hDPPIV with 273 water molecules [9], in this study, due to better resolution (1.9 Å), we identified 1468 water molecules around apo hDPPIV. In addition, we found one glycerol molecule per active site in a dimer (**Fig. 1**). The glycerol molecule is located around the S1 site, and is assumed to be derived from the cryo-protectant. The hydroxyl group (OH1) of the glycerol molecule forms hydrogen bonds with the hydroxyl group (Oη) of Tyr547 and the N–H group of Tyr631. The other two hydroxyl groups (OH2 and OH3) of the glycerol molecule form electrostatic interaction with one of the sodium ions. In physiological conditions, the positions of the hydroxyl groups of the glycerol molecule are considered to be occupied by water molecules. There were only three water molecules around the active site of apo hDPPIV at 2.6 Å resolution in our previous report [9]. However, in this high-resolution crystal structure, many water molecules, forming a close hydrogen bond network, were around the active site. We focused on 10 water molecules, which existed around the active site in the A and B molecules in the dimer of hDPPIV, and defined them as W1–W10 for convenience (**Table 2**). **Fig. 1** shows a schematic view of the hydrogen bond network around the active site including the 10 water molecules and a glycerol molecule. There is a hydrogen bond network between Oε2 of Glu206 and Oη of Tyr547 through four water molecules (W1, W2, W3, and W4).

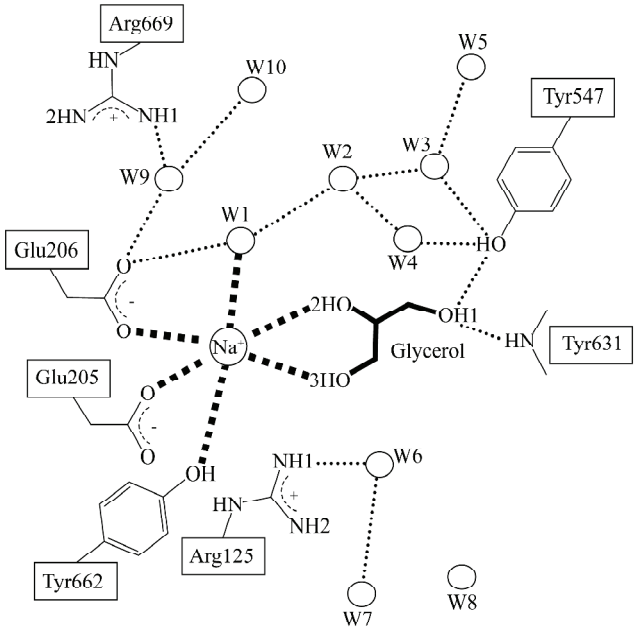

Fig. 1 Schematic view of the binding modes of a glycerol molecule and a sodium ion around the active site of apo human dipeptidyl peptidase IV

Hydrogen bonds are indicated by thin dotted lines. Electrostatic interactions around the sodium ion are indicated by thick dotted lines. W1–W10 represent ordered water molecules.

In the course of apo hDPPIV crystal structure determination, an unknown electron density existed in the proximity of Glu205 and Glu206, which are important for

Table 2 Summary of water molecules around the active site of apo human dipeptidyl peptidase IV and complexed human dipeptidyl peptidase IV

	W1	W2	W3	W4	W5	W6	W7	W8	W9	W10
Apo										
1.8 Å high resolution										
Mol-A	Wat770	Wat306	Wat176	Wat646	Wat217	Wat691	Wat722	Wat638	Wat87	Wat617
Mol-B	Wat1195	Wat985	Wat925	Wat1164	Wat837	Wat1317	Wat1396	Wat1429	Wat787	Wat1196
2.6 Å resolution (PDB code: 1J2E)										
Mol-A	–	–	–	–	–	Wat14	–	–	Wat89	–
Mol-B	–	–	–	–	Wat194	Wat6	–	–	Wat143	–
Peptide										
Diprotin B										
Mol-A	–	–	Wat581	–	Wat496	–	Wat70	Wat217	Wat4	Wat184
Mol-B	–	–	Wat630	–	Wat876	–	Wat643	Wat820	Wat636	Wat587
Diprotin A (PDB code: 1WCY)										
Mol-A	–	–	Wat174	–	Wat215	–	Wat586	Wat585	Wat87	Wat580
Mol-B	–	–	Wat755	–	Wat670	–	Wat214	Wat213	Wat621	–

–, No atoms; Mol-A, A molecule; Mol-B, B molecule; PDB, Protein Data Bank.

recognition of substrate N-terminus in the A molecule of the dimer. This electron density was also observed in the B molecule of the dimer. According to general refinement procedure, we first assumed that this unknown electron density was a water molecule. Previous reports on the structure of apo hDPPIV have also indicated the existence of a water molecule at the same position [12,15,17]. The unknown electron density has six nearest-neighbors, that is, three oxygen atoms from the protein, two oxygen atoms from the glycerol molecule, and one water molecule in an octahedral geometry. Distances from the unknown electron density to the six nearest-neighbors are short (2.43–3.04 Å); the distance between the unknown electron density and Oη of Tyr662 is too short (2.43 Å). Under our crystallization conditions, sodium acetate was used as an additive reagent. The distance expected for an Na^+–O pair in an octahedral coordination shell is 2.46 Å. Therefore, we concluded that the unknown electron density is a sodium ion and defined the sodium ions as Na-1 and Na-2.

Previously, Nayal and Di Cera raised the possibility that some water molecules in coordinates deposited in the Protein Data Bank (PDB) were in fact sodium ions [35]. They proposed to calculate V_{Na+} for the water molecules in PDB coordinates. V_{Na+} can be calculated from the distance and bond order between a water molecule and neighboring atom. It has been reported that the average value of V_{Na+} for a water molecule is 0.18 valence units (v.u.), with a standard deviation of 0.13 v.u.. If V_{Na+} is approximately 0.18 v.u., the assignment of a water molecule is correct. However, if V_{Na+} is considerably larger than the average value, the presumed water molecule could be another atom. We calculated the V_{Na+} value of the unknown electron density in our structure of apo hDPPIV in both the A and B molecules of the dimer. The values found (0.85 v.u. and 0.90 v.u., respectively) were much higher than the average value of V_{Na+} (0.18 v.u.). These findings support our identification of the unknown electron density as a sodium ion.

As a result of V_{Na+} calculation for other water molecules in the overall structure of the apo hDPPIV dimer, we found two water molecules with high V_{Na+} (0.70 v.u. and 0.97 v.u.). As these values were also much higher than the average value of V_{Na+} (0.18 v.u.), we assigned these molecules as sodium ions (Na-3 and Na-4) based on the distance and geometric arrangement around the oxygen atoms. Na-3 was located in the neighborhood of the non-crystallographic symmetry axis. There were six oxygen atoms around the Na-3 ion, two oxygen atoms from Oε1 of Gln731 in the dimer, and four oxygen atoms from water molecules. Na-4 interacted with five oxygen atoms in the contact area of neighboring molecules. Four of these oxygen atoms were from the protein, that is, carbonyl oxygens of Gly490 and Leu491 in the B molecule, carbonyl oxygens of Val279 and Leu276 in the A molecule after a symmetry operation (-x+1/2+1, -y+1, z+1/2), and one oxygen atom was from a water molecule. Distances from

Na-4 to the oxygen atoms were very short (2.23–2.47 Å).

Crystal structure of hDPPIV-diprotin B complex

In the crystal structure of the hDPPIV-diprotin B complex determined in this study, we found one diprotin B per active site in a dimer. The diprotin B was non-covalently bound to Ser630 of the catalytic triad as well as diprotin A. As diprotin B is also a slowly hydrolysable substrate [27], structures with a non-covalent binding mode might reflect a molecular recognition state. The electron density map around diprotin B and schematic view of the binding mode of diprotin B are shown in **Figs. 2(A)** and **2(B)**, respectively. The electron densities for the side-chain of Leu-3 were weak, because their B-factor values were relatively high in comparison with the other atoms in diprotin B. In each molecule of the asymmetric unit, no difference in conformation was seen between the two hDPPIV molecules. The root-mean-square deviation (RMSD) between apo hDPPIV and the hDPPIV-diprotin B complex for the corresponding Cα atoms was 0.19 Å. In order to identify the location of sodium ions, we subsequently calculated V_{Na+} values for all water molecules in the determined crystal structure of the hDPPIV-diprotin B complex. As a result, V_{Na+} values of the two water molecules were 0.76 v.u. and 0.94 v.u., respectively. Therefore, we assumed that these two presumably water molecules were

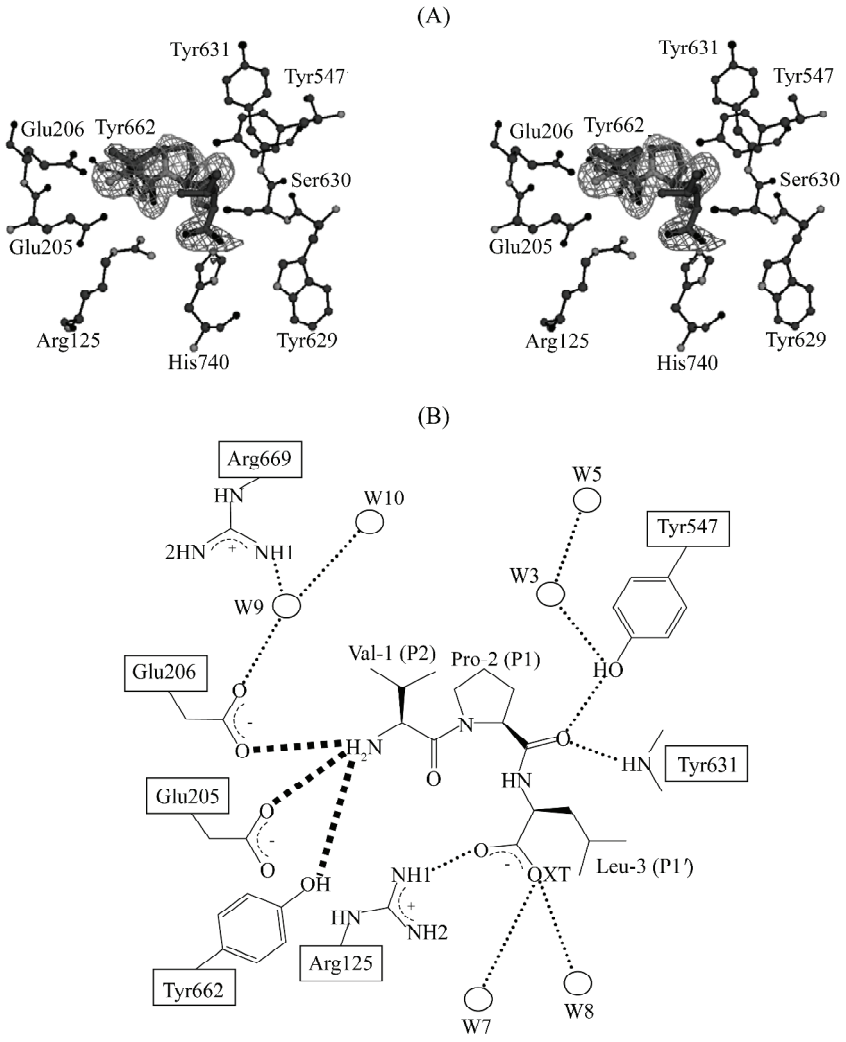

Fig. 2 Diprotin B bound to the active site of human dipeptidyl peptidase IV (hDPPIV)

(A) Stereo image of the difference in electron density map contoured at 3.5 σ. hDPPIV is shown by the ball-and-stick model, diprotin B is shown by the stick mdel. (B) Schematic view of the binding mode of diprotin B to the active site of hDPPIV. The dash lines indicate potential hydrogen bonds and electrostatic interaction. Water molecules are indicated by W3, W5, W7, W8, W9 and W10.

in fact sodium ions. These sodium ions were found at the same position as Na-3 and Na-4 in apo hDPPIV. In addition, the sodium ion (Na-4) was located at the same position in the crystal structures of apo hDPPIV, hDPPIV-diprotin B complex, and previously published hDPPIV [19]. Moreover, the crystal lattice of these structures was the same. These results suggest that Na-4 is essential for crystal contact with a neighboring molecule in this crystal lattice.

Difference in binding mode to hDPPIV between diprotin B and diprotin A

The RMSD between the hDPPIV-diprotin B complex and the hDPPIV-diprotin A complex [10] for corresponding Cα atoms was 0.17 Å. No difference in conformation of the overall DPPIV molecule between the two complex molecules was observed. However, interactions of diprotin B with hDPPIV at S1' and S2 sites were different from those of diprotin A.

At the S1' site, the phenol ring of Tyr547 was located near the side-chain of P1' parts of diprotin B and diprotin A. The closest atom of the benzene ring was Cβ in both diprotin B (Leu-3) and diprotin A (Ile-3). Comparison of the distance from Cβ of diprotin B and diprotin A to each atom of the side-chain of Tyr547 revealed that the distance between Cβ (Leu-3) and Oη of Tyr547 was the shortest of all distances. This result suggests that interaction between the side-chain of Tyr547 and Cβ of diprotin B (or diprotin A) is C - H· · ·O interaction rather than a hydrophobic interaction between carbon atoms. C - H· · ·O interaction, which has been widely accepted to contribute to the stability of interactions in small-molecule structures [39–41]. Moreover, short C - H· · ·O interaction has already been reported in a number of known protein structures [42]. We calculated the positions of hydrogen atoms of Cβ in both diprotin B and diprotin A using the program CNX as described before [42]. As a result, the position of hydrogen atoms of Cβ in diprotin B was quite different from that in diprotin A. The Cβ - H· · ·Oη (Tyr547) angle was also different between diprotin B and diprotin A. In diprotin B (Leu-3), Cβ had two additional hydrogen atoms (H1 and H2). Cβ - H1· · ·Oη angles of the A molecule and B molecule in the dimer were 89.1° and 68.8°, respectively, and Cβ - H2· · ·Oη angles were 124.1° and 158.1°, respectively. However, Cβ of diprotin A (Ile-3) had only one additional hydrogen atom, which was directed towards Oη of Tyr547. The Cβ - H· · ·Oη angles in the dimer were 175.3° and 174.2°, respectively. Therefore, Cβ of diprotin A (Ile-3), the hydrogen atom of diprotin A, and Oη of Tyr547 are in line. These results suggest that Cβ of diprotin A (Ile-3) formed a stronger interaction with Oη of Tyr547 than Cβ of diprotin B (Leu-3).

In addition to the C - H· · ·O interaction, hydrophobic interactions were observed at the S1' site. In Leu-3 of diprotin B, only Cδ1 was close to Cζ of the benzene ring of Tyr547 (A molecule, 3.69 Å; B molecule, 4.41 Å). However, in Ile-3 of diprotin A, two carbon atoms (Cγ1 and Cδ1) were close to Cε1 and Cζ of the benzene ring of Tyr547 (A molecule, 3.56 Å and 3.94 Å; B molecule, 3.59 Å and 3.90 Å). At the S2 site, the side-chain of both diprotin B (Val-1) and diprotin A (Ile-1) was located near the benzene ring of Phe357. The distance between Cδ of diprotin A (Ile-1) and C2 of Phe357 was shorter than that between Cγ2 of diprotin B (Val-1) and Cδ2 of Phe357 (4.10 Å and 3.85 Å in dimer vs. 4.74 Å and 4.61 Å in dimer). The average value of the accessible surface areas (ASA) between hDPPIV and diprotin B in dimer was 590.2 Å^2, as given by Lee and Richards [43]. In contrast, the average value of ASA between hDPPIV and diprotin A in dimer was 616.7 Å^2. Therefore, it is assumed that diprotin A interacts more potently with hDPPIV than diprotin B.

Using an enzymatic assay, a previous study that examined DPPIV substrate specificity for tripeptides, including diprotin A and diprotin B, showed K_m values of $(1.6\pm0.1)\times10^{-5}$ M and $(0.4\pm0.05)\times10^{-5}$ M for diprotin B and diprotin A, respectively [27]. The study also showed that tripeptides having an Ile residue at the P1′ site show low Km values compared with those having a Leu residue. These biochemical findings can be explained on the basis of our structural information of hDPPIV.

Insights for design of potent hDPPIV inhibitors

To examine interactions between hDPPIV and diprotin B and to elucidate the function of water molecules around the active site, the crystal structures of hDPPIV determined in this study were superimposed on reported apo hDPPIV structures [12,13,15,17]. Comparison of the S2, S1, and S1′ sites among the crystal structures can be summarized as follows.

S2 site The position of the nitrogen atom of Val-1 in diprotin B was occupied by a sodium ion in apo hDPPIV (**Fig. 3**, position A). The sodium ion interacted similarly with the oxygen atoms of Glu205, Glu206, and Tyr662. The carbonyl oxygen of Val-1 was located at the position of OH3 of the glycerol molecule in apo hDPPIV (**Fig. 3**, position B) and at the position of a water molecule in the other apo structures [15,17]. In apo hDPPIV and the hDPPIV-diprotin B complex determined in this study, the water molecule (W9) formed three hydrogen bonds with Oε2 of Glu206, Nη1 of Arg669, and W10 [**Fig. 2(B)**]. This water molecule (W9) is conserved in reported apo

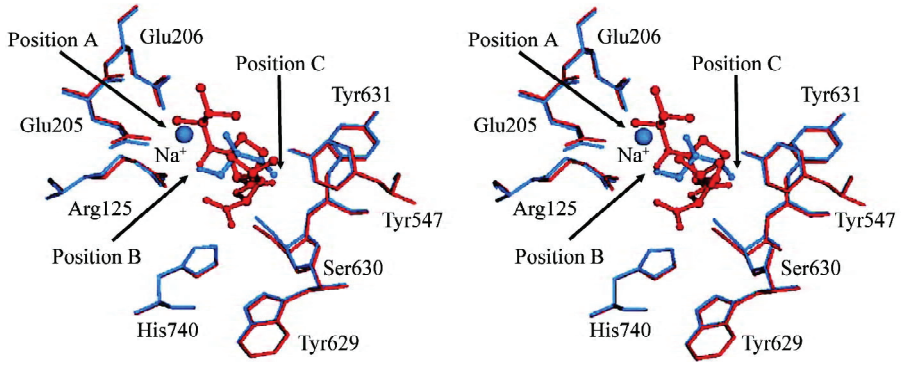

Fig. 3 Stereo view of superposition of human dipeptidyl peptidase IV (hDPPIV)-diprotin B complex and apo hDPPIV around the active sites

The structures of the hDPPIV-diprotin B complex and apo hDPPIV are shown in red and blue, respectively.

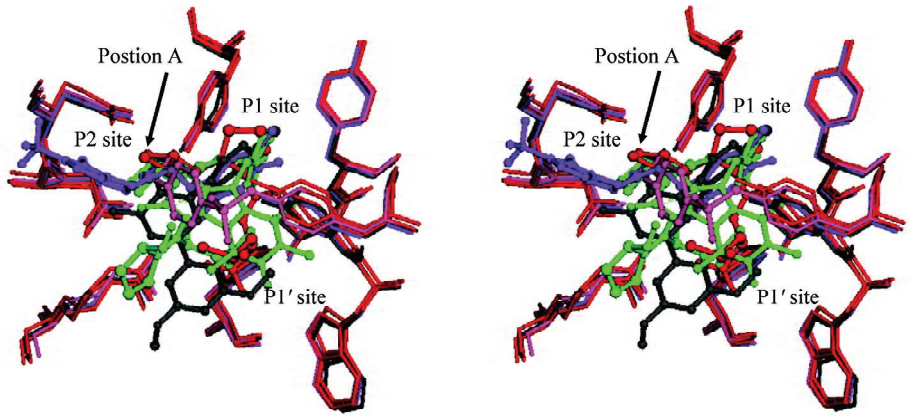

Fig. 4 Stereo view of superimposition of human dipeptidyl peptidase IV (hDPPIV)-diprotin B complex (red), 1RWQ (silver), 1X70 (purple), 2GBR (orange), 2AJ8 (green) and 2AJC (pink) around the active sites

DPPIV and ligands are shown by the stick and the ball-and-stick model, respectively.

structures, although crystallization conditions and the space group are completely different [12,15,17].

S1 site The carbonyl oxygen of Pro-2 in diprotin B was located at the oxyanion hole, and formed two hydrogen bonds with Oη of Tyr547 and the nitrogen atom of Tyr631 (**Fig. 3**, position C). In apo hDPPIV, OH1 of the glycerol molecule was located at the same position as the carbonyl oxygen of Pro-2, and interacted with neighboring atoms in the same manner as the carbonyl oxygen of Pro-2. In addition, the water molecule (W3) formed a hydrogen bond with Oη of Tyr547 in our and other apo hDPPIV structures [12,13,17].

S1′ site The oxygen atom of Leu-3 in diprotin B formed a hydrogen bond with Nη1 of Arg125. In the crystal structures of apo hDPPIV, the water molecule (W6) existed in place of the oxygen atom of Leu-3 and interacted with Nη1 of Arg125.

From these comparisons we conclude that positively charged functional groups in position A, the oxygen atoms in positions B and C, and conserved water molecules (W3 and W9) play important roles in ligands' interaction with hDPPIV. Introduction of positively charged groups, such as amino and imide groups in position A and replacement of the water molecules by oxygen-containing groups, such as hydroxy and carbonyl groups, will lead to improvement of the inhibitory activity of ligands. As a result of the comparison of DPPIV complexed structures with inhibitors/substrates, which were determined beyond 2.2 Å resolution, position A was occupied by positively charged groups (**Fig. 4**). These findings are useful for the design

of potent hDPPIV inhibitors.

Acknowledgements

We thank Dr. Y. KATSUYA and staff of SPring-8 BL32B2, for their assistance in collecting diffraction data.

References

1 Hopsu-Havu VK, Glenner GG. A new dipeptide naphthylamidase hydrolyzing glycyl-prolyl-beta-naphthylamide. Histochemie 1966, 7: 197–201
2 De Meester I, Korom S, Van Damme J, Scharpé S. CD26, let it cut or cut it down. Immunol Today 1999, 20: 367–375
3 Bednarczyk JL, Carroll SM, Marin C, McIntyre BW. Triggering of the proteinase dipeptidyl peptidase IV (CD26) amplifies human T lymphocyte proliferation. J Cell Biochem 1991, 46: 206–218
4 Ajami K, Abbott CA, Obradovic M, Gysbers V, Kähne T, MaCaughan GW, Gorrell MD. Structural requirements for catalysis, expression, and dimerization in the CD26/DPIV gene family. Biochemistry 2003, 42: 694–701
5 Blanco J, Valenzuela A, Herrera C, Lluís C, Hovanessian AG, Franco R. The HIV-1 gp120 inhibits the binding of adenosine deaminase to CD26 by a mechanism modulated by CD4 and CXCR4 expression. FEBS Lett 2000, 477: 123–128
6 Mentlein R, Gallwitz B, Schmidt WE. Dipeptidyl-peptidase IV hydrolyses gastric inhibitory polypeptide, glucagon-like peptide-1 (7-36) amide, peptide histidine methionine and is responsible for their degradation in human serum. Eur J Biochem 1993, 214: 829–835
7 Marguet D, Baggio L, Kobayashi T, Bernard AM, Pierres M, Nielsen PF, Ribel U *et al*. Enhanced insulin secretion and improved glucose tolerance in mice lacking CD26. Proc Natl Acad Sci USA 2000, 97: 6874–6879
8 Ahrén B, Simonsson E, Larsson H, Landin-Olsson M, Torgeirsson H, Jansson PA, Sandqvist M *et al*. Inhibition of dipeptidyl peptidase IV improves metabolic control over a 4-week study period in type 2 diabetes. Diabetes Care 2002, 25: 869–875
9 Hiramatsu H, Kyono K, Higashiyama Y, Fukushima C, Shima H, Sugiyama S, Inaka K *et al*. The structure and function of human dipeptidyl peptidase IV (DPPIV), possessing a unique eight-bladed β-propeller fold. Biochem Biophys Res Commun 2003, 302: 849–854
10 Hiramatsu H, Yamamoto A, Kyono K, Higashiyama Y, Fukushima C, Shima H, Sugiyama S *et al*. The crystal structure of human dipeptidyl peptidase IV (DPPIV) complex with diprotin A. Biol Chem 2004, 385: 561–564
11 Rasmussen HB, Branner S, Wiberg FC, Wagtmann N. Crystal structure of human dipeptidyl peptidase IV/CD26 in complex with a substrate analog. Nature Struct Biol 2003, 10: 19–25
12 Engel M, Hoffmann T, Wagner L, Wermann M, Heiser U, Kiefersauer R, Huber R *et al*. The crystal structure of dipeptidyl peptidase IV (CD26) reveals its functional regulation and enzymatic mechanism. Proc Natl Acad Sci USA 2003, 100: 5063–5068
13 Thoma R, Löffler B, Stihle M, Huber W, Ruf A, Henning M. Structural basis of proline-specific exopeptidase activity as observed in human dipeptidyl peptidase-IV. Structure 2003, 11: 947–959
14 Oefner C, D'Arcy A, Mac Sweeney A, Pierau S, Gardiner R, Dale GE. High-resolution structure of human apo dipeptidyl peptidase IV/CD26 and its complex with 1-[([2-[(5-iodopyridin-2-yl) amino]-ethyl]amino)-acetyl]-2-cyano-(S)-pyrrolidine. Acta Crystallogr D 2003, 59: 1206–1212
15 Aertgeerts K, Ye S, Tennant MG, Kraus ML, Rogers J, Sang BC, Skene RJ *et al*. Crystal structure of human dipeptidyl peptidase IV in complex with a decapeptide reveals details on substrate specificity and tetrahedral intermediate formation. Protein Sci 2004, 13: 412–421
16 Peters JU, Weber S, Kritter S, Weiss P, Wallier A, Boehringer M, Hennig M *et al*. Aminomethylpyrimidines as novel DPP-IV inhibitors: A 10(5)-fold activity increase by optimization of aromatic substituents. Bioorg Med Chem Lett 2004, 14: 1491–1493
17 Bjelke JR, Christensen J, Branner S, Wagtmann N, Olsen C, Kanstrup AB, Rasmussen HB. Tyrosine 547 constitutes an essential part of the catalytic mechanism of dipeptidyl peptidase IV. J Biol Chem 2004, 279: 34691–34697
18 Weihofen WA, Liu J, Reutter W, Saenger W, Fan H. Crystal structure of CD26/dipeptidyl-peptidase IV in complex with adenosine deaminase reveals a highly amphiphilic interface. J Biol Chem 2004, 279: 43330–43335
19 Kim D, Wang L, Beconi M, Eiermann GJ, Fisher MH, He H, Hickey GJ *et al*. (2R)-4-oxo-4-[3-(trifluoromethyl)-5,6-dihydro[1,2,4]triazolo[4,3-a]pyrazin-7(8H)-yl]-1-(2,4,5-trifluorophenyl)butan-2-amine: A potent, orally active dipeptidyl peptidase IV inhibitor for the treatment of type 2 diabetes. J Med Chem 2005, 48: 141–151
20 Weihofen WA, Liu J, Reutter W, Saenger W, Fan H. Crystal structures of HIV-1 Tat-derived nonapeptides Tat-(1-9) and Trp2-Tat-(1-9) bound to the active site of dipeptidyl-peptidase IV (CD26). J Biol Chem 2005, 280: 14911–14917
21 Qiao L, Baumann CA, Crysler CS, Ninan NS, Abad MC, Spurlino JC, Desjarlais R *et al*. Discovery, SAR, and X-ray structure of novel biaryl-based dipeptidyl peptidase IV inhibitors. Bioorg Med Chem Lett 2006, 16: 123–128
22 Engel M, Hoffmann T, Manhart S, Heiser U, Chambre S, Huber R, Demuth HU *et al*. Rigidity and flexibility of dipeptidyl peptidase IV: Crystal structures of and docking experiments with DPIV. J Mol Biol 2006, 355: 768–783
23 Nordhoff S, Cerezo-Galvez S, Feurer A, Hill O, Matassa VG, Metz G, Rummey C *et al*. The reversed binding of β-phenethylamine inhibitors of DPP-IV: X-ray structures and properties of novel fragment and elaborated inhibitors. Bioorg Med Chem Lett 2006, 16: 1744–1748
24 Nakasako M. Large-scale networks of hydration water molecules around bovine β-trypsin revealed by cryogenic X-ray crystal structure analysis. J Mol Biol 1999, 289: 547–564
25 Zhang Z, Komives EA, Sugio S, Blacklow SC, Narayana N, Xuong NH, Stock AM *et al*. The role of water in the catalytic efficiency of triosephosphate isomerase. Biochemistry 1999, 38: 4389–4397
26 Bhat TN, Bentley GA, Boulot G, Greene MI, Tello D, Dall'Acqua W, Souchon H *et al*. Bound water molecules and conformational stabilization help mediate an antigen-antibody association. Proc Natl Acad Sci USA 1994, 91: 1089–1093
27 Rahfeld J, Schierhorn M, Hartrodt B, Neubert K, Heins J. Are diprotin A (Ile-Pro-Ile) and diprotin B (Val-Pro-Leu) inhibitors or substrates of dipeptidyl peptidase IV? Biochim Biophy Acta 1991, 1076: 314–316
28 Umezawa H, Aoyagi T, Ogawa K, Naganawa H, Hamada M, Takeuchi T. Diprotins A and B, inhibitors of dipeptidyl aminopeptidase IV, produced by bacteria. J Antibiotics 1984, 37: 422–425
29 Hiramatsu H, Kyono K, Shima H, Fukushima C, Sugiyama S, Inaka K, Yamamoto A *et al*. Crystallization and preliminary X-ray study of human dipeptidyl peptidase IV. Acta Crystallogr D 2003, 59: 595–596
30 Leslie AGW. Recent changes to the MOSFLM package for processing film and image plate data. Joint CCP4 ESF-EAMCB Newsl Protein Crystallogr 1992, 26: 22–33
31 Collaborative Computational Project Number 4. The CCP4 suite: Programs for protein crystallography. Acta Crystallogr D 1994, 50: 760–763
32 Brünger AT, Adams PD, Clore GM, Delano WL, Gros P, Grosse-Kunstleve

RW, Jiang JS *et al*. Crystallography and NMR system: A new software suite for macromolecular structure determination. Acta Crystallogr D 1998, 54: 905–921

33 Laskowski RA. Procheck: A program to check the stereochemical quality of protein structures. J Appl Crystallogr 1993, 26: 283–291

34 Kleywegt GJ, Jones TA. Halloween ... Masks and bones. In: Bailey S, Hubbard R, Waller D eds. From First Map to Final Model. SERC Daresbury Laboratory. Warrington, 1994: 59–66

35 Nayal M, Di Cera E. Valence screening of water in protein crystals reveals potential Na^+ binding sites. J Mol Biol 1996, 256: 228–234

36 Brown ID, Wu KK. Empirical parameters for calculating cation-oxygen bond valence. Acta Crystallogr B 1976, 32: 1957–1959

37 Brown ID. Chemical and steric constraints in inorganic solids. Acta Crystallogr B 1992, 48: 553–572

38 Nayal M, Di Cera E. Predicting Ca^{2+}-binding sites in proteins. Proc Natl Acad Sci USA 1994, 91: 817–821

39 Sutor DJ. The C- H· · ·O hydrogen bond in crystals. Nature 1962, 195: 68–69

40 Taylor R, Kennard O. Crystallographic evidence for the existence of C- H· · ·O, C- H· · ·N, and C- H· · ·Cl hydrogen bonds. J Am Chem Soc 1982, 104: 5063–5070

41 Steiner T, Saenger W. Role of C- H· · ·O hydrogen bonds in the coordination of water molecules. J Am Chem Soc 1993, 115: 4540–4547

42 Derewenda ZS, Lee L, Derewenda U. The occurrence of C-H· · ·O hydrogen bonds in proteins. J Mol Biol 1995, 252: 248–622

43 Lee B, Richards FM. The interaction of protein structures: Estimation of static accessibility. J Mol Biol 1971, 55: 379–400

Edited by
Michael HENNIG